The winter Arctic Oscillation and the timing of snowmelt in Europe

Kevin Schaefer, A. Scott Denning, and Owen Leonard

Department of Atmospheric Science, Colorado State University, Fort Collins, Colorado, USA

Received 16 July 2004; revised 10 September 2004; accepted 7 October 2004; published 20 November 2004.

[1] Observations indicate earlier spring snowmelt in the northern hemisphere. We hypothesize that increased temperatures and decreased precipitation due to a positive trend in the winter Arctic Oscillation (AO) have advanced the date of snowmelt. To test this, we modeled snowmelt using the Simple Biosphere model, Version 2 (SiB2) and the National Centers for Environmental Prediction (NCEP) reanalysis from 1958–2002. The simulated snowmelt dates are consistent with dates derived from National Oceanic and Atmospheric Administration (NOAA) weekly snow charts. The winter AO exerts the strongest influence on the timing of snowmelt in northern Europe, with a weaker influence in eastern Siberia and almost no influence in North America. The winter AO trend can statistically explain 20–70% of simulated snowmelt trends in northern Europe. *INDEX TERMS:* 1620 Global Change: Climate dynamics (3309); 1655 Global Change: Water cycles (1836); 1610 Global Change: Atmosphere (0315, 0325); 1863 Hydrology: Snow and ice (1827). **Citation:** Schaefer, K., A. S. Denning, and O. Leonard (2004), The winter Arctic Oscillation and the timing of snowmelt in Europe, *Geophys. Res. Lett.*, *31*, L22205, doi:10.1029/2004GL021035.

1. Introduction

[2] Based on station measurements and National Oceanic and Atmospheric Administration (NOAA) weekly snow charts, the date of spring snowmelt in the northern hemisphere spring has advanced 9–15 days between 1972–2000 [*Dye*, 2002]. The northern hemisphere winters have become warmer [*Serreze et al.*, 2000] and spring temperatures and cloud cover have increased [*Stone et al.*, 2002], advancing the date of snowmelt [*Cutforth et al.*, 1999; *Zhou et al.*, 2001; *Dye*, 2002]. High latitude winter snow depths have declined and spring snow cover has decreased 10% [*Serreze et al.*, 2000; *Dye*, 2002; *Stone et al.*, 2002]. Latitudes north of 55–60°N show the strongest trends towards earlier snowmelt [*Dye*, 2002] while Siberia shows increased snow depth and delayed snowmelt [*Stone et al.*, 2002].

[3] The Arctic Oscillation (AO) is a zonally symmetric seesaw in atmospheric mass between the Arctic and mid-latitudes. Positive AO polarity has less mass and lower pressure in the Arctic and more mass and higher pressure at 45°N. Geostrophic balance results in a north-south dipole in the strength of the zonal wind between 25°N and 60°N. Positive AO polarity is associated with stronger westerly winds north of 45°N and weaker winds south of 45°N. The AO is strongest and most variable in winter, when radiative cooling is greatest and the polar vortex is strongest. The AO weakens in March as convection over land breaks down the polar vortex. The AO randomly switches polarity with a characteristic synoptic time scale of 7–10 days [*Thompson et al.*, 2000; *Thompson and Wallace*, 2000, 2001].

[4] Since the 1950s, the winter AO has exhibited a trend towards positive polarity [*Thompson et al.*, 2000], indicating a gradual strengthening of the wintertime polar vortex [*Serreze et al.*, 2000]. At mid to high northern latitudes, the AO statistically explains ~31% of the winter temperature variance [*Serreze et al.*, 2000] and ~40% of the winter temperature trends [*Thompson et al.*, 2000].

[5] We hypothesize that the trend towards earlier spring snowmelt results from the winter AO trend. The date of spring snowmelt depends on the cumulative effects of precipitation, temperature, and cloud cover [*Dye*, 2002; *Stone et al.*, 2002]. Increased precipitation in winter delays snowmelt by increasing the total energy required for melting [*Cutforth et al.*, 1999; *Vaganov et al.*, 1999; *Stone et al.*, 2002]. Warmer temperatures and increased cloudiness in spring advance snowmelt by increasing melting and sublimation rates [*Stone et al.*, 2002]. Increased temperatures and decreased precipitation from a positive winter AO trend can explain earlier snowmelt.

2. Methods

[6] To test our hypothesis, we used the National Centers for Environmental Prediction/National Center for Atmospheric Research (NCEP/NCAR) reanalysis [*Kalnay et al.*, 1996] and the Simple Biosphere model, Version 2 (SiB2) [*Sellers et al.*, 1996] to model the winter snow pack and the date of snowmelt. We compared simulated snowmelt dates with observed dates derived from NOAA weekly snow charts and used simple statistical techniques to relate simulated snowmelt to the winter AO. SiB2 is a land surface model, so we did not include AO effects on the ocean.

[7] SiB2 is a biophysical model, which means it models the biological processes of photosynthesis and respiration and the physical processes of turbulent transfer of latent and sensible heat. As prognostic variables, SiB2 predicts moistures and temperatures of the canopy, canopy air space, and soil [*Sellers et al.*, 1996]. SiB2 tracks snow depth assuming a single snow layer with a constant snow density of 0.25 g cm^{-3} accounting for canopy interception of precipitation, melting, sublimation, runoff, and phase changes [*Bonan*, 1996]. SiB2 uses a linear version of the fractional snow cover model from the Common Land Model [*Dai et al.*, 2003]: for snow depths less than 6 cm, the snow cover fraction increases linearly from zero to one. For snow depths greater than 6 cm, SiB2 assumes a snow cover fraction of one.

[8] We defined snowmelt as the date when the fractional snow cover falls below 25% (snow depth of 1.5 cm), which roughly corresponds to the end of spring runoff [*Cutforth et*

0094-8276/04/2004GL021035$05.00

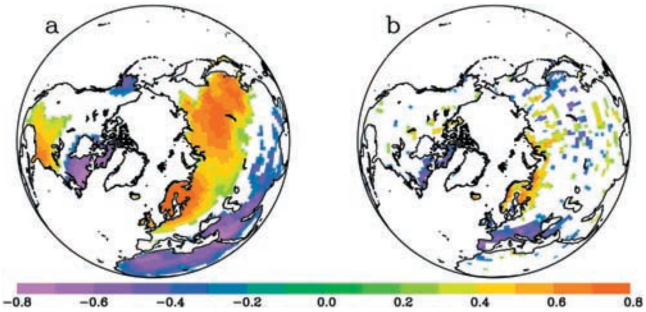

Figure 1. Correlations between the average JFM AO index and average JFM NCEP (a) temperature and (b) precipitation.

al., 1999]. For pixels where it never snows (snowmelt undefined), the snowmelt date is set to January 1. Pixels with intermittent snow (snowmelt defined in some years, but not others) typically show statistically significant trends with no physical meaning. We confined our analysis to those pixels where snowmelt is defined nearly every year by omitting all pixels whose 45-year average snowmelt fell in January.

[9] Observed snowmelt dates come from NOAA weekly snow cover charts for 1967–2000 resampled onto a 0.25 × 0.25° grid [*Armstrong and Brodzik*, 2002]. Based on visible satellite reflectances, each chart covers a 7-day period with each pixel either completely covered or completely free of snow. The instrument swaths in the original charts do not line up with the NCEP grid, so resampling preserves as much spatial information as possible. The effective spatial resolution of the resampled dataset is 120–200 km. Each NCEP pixel contained approximately 16 snow chart pixels, from which we estimated the observed fractional snow cover. We calculated the observed snowmelt date as the middle of the 7-day period when the snow cover fraction fell below 25%. The minimum accuracy of snowmelt date calculated in this manner is ±3.5 days. Low solar illumination, high zenith angle, dense forest cover, and cloud cover can result in higher uncertainty [*Dye*, 2002].

[10] As input weather, we used the NCEP reanalysis from 1958–2002. The NCEP reanalysis estimates surface temperature, pressure, wind speed, precipitation, and radiation every 6 hours on a 1.875° by 1.904° Gaussian grid. The estimated NCEP snow cover is "nudged" by observed snow cover data derived from the same visible reflectances used in the NOAA weekly snow charts, so simulating snowmelt with SiB2 allowed us to use the snow charts for independent validation. We linearly interpolated in time between the NCEP data points to the SiB2 10-minute time step. Other inputs are as described by *Schaefer et al.* [2002] and *Schaefer* [2004].

[11] We represented the AO with an index based on the first principal component of NCEP sea level pressure [*Thompson and Wallace*, 2000]. Our analysis focused on January-February-March (JFM), when the AO shows the strongest trends. Figure 1 correlates the average JFM AO index with the average JFM NCEP surface air temperature and precipitation. Smoother zonal flow associated with positive AO polarity favors advection of warm, moist oceanic air deep into continental interiors, resulting in higher temperatures. Positive AO polarity shifts the Atlantic storm tracks northward, increasing precipitation in Eurasia north of 55°N. Positive AO polarity decreases the number of cold air outbreaks in central North America, resulting in positive temperature anomalies. Cold, dry airflow from the Arctic results in negative temperature and precipitation correlations in Alaska and northeast Canada [*Thompson and Wallace*, 2000, 2001].

[12] We related snowmelt to the AO using standard correlations, regressions, and trends. For the AO index, we first averaged over JFM, then removed the long-term trend, and lastly removed the long-term JFM mean. For snowmelt, we removed the long-term trends and then the long-term means. This resulted in a time series of detrended, annual anomalies from which we calculated correlations and regressions. We omitted trends, correlations, and regressions failing a single-tail student T-test at 95% significance. The degrees of freedom for the T-test were based on the number of years (45 years for simulated snowmelt and 34 years for observed snowmelt).

3. Results

[13] Figure 2 shows the mean day-of-year of simulated snowmelt for 1958–2002. Removing all the mean snowmelt dates that fall in January creates a snow line at ~40°N, south of which, snowfall does not occur every year or never occurs at all.

[14] Figure 3 shows the mean of observed minus simulated snowmelt for 1967–2000. The differences between observed and simulated snowmelt along the Arctic Ocean coastline and the alternating positive and negative differences spanning Siberia probably result from errors in the NCEP reanalysis precipitation. NCEP predicts low precipitation along the Arctic coastline, resulting in earlier snowmelt than observed. The wave-like pattern in Siberia is probably a numerical artifact: the spectral representation of continuous fields produces alternating dry and wet regions across Siberia when in reality the precipitation, and thus snowmelt date, is fairly uniform. Large differences of ±35 days in the Rockies, Himalayas, and Alps probably result from errors in the snow cover charts, which show unrealistically large variability in snowmelt date, with standard deviations of ±20–50 days. Overall, however, the simulated snowmelt generally occurs within ±15 days of observed snowmelt for most of the land regions.

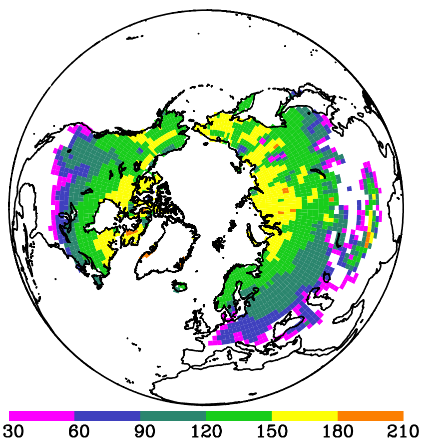

Figure 2. The mean simulated snowmelt dates (day) for 1958–2002.

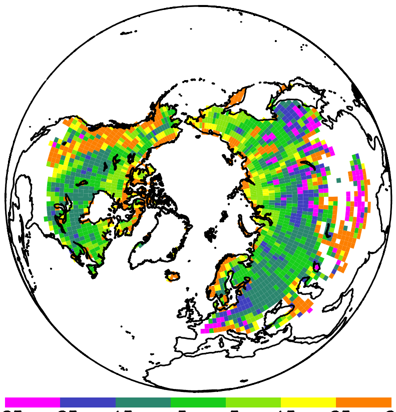

Figure 3. The mean of observed minus simulated snowmelt dates (day) for 1967–2000.

[15] The simulated and observed snowmelt dates negatively correlate with the average JFM AO index for 1967–2000 in Northern Europe (Figure 4) where positive AO polarity increases temperature, but has little or no effect on precipitation, resulting in earlier snowmelt. Although clearly weaker than in Europe, the snowmelt dates also negatively correlate with the JFM AO in eastern Siberia. We saw no significant connection with the AO in northeast Canada: for positive AO polarity, snowmelt delays due to colder temperatures cancel advances due to decreased precipitation. Much of the temperature increases due to positive AO polarity in central and southeast North America lie south of the snow line, so we see only scattered correlations with snowmelt. Overall, the AO strongly influences snowmelt in northern Europe, with a weaker influence in eastern Siberia and almost no influence in North America.

[16] Simulated snowmelt trends for 1958–2002 (Figure 5) show advances of 0.3–0.5 day year^{-1}, consistent with *Dye* [2002], but did not reflect observed delays in Siberia [*Stone et al.*, 2002] and advances in Alaska [*Dye*, 2002]. The congruent trend fraction [*Thompson et al.*, 2000] statistically quantifies how much of the snowmelt trends result from the AO trend:

$$x = \left| r \frac{t_{AO}}{t_{snowmelt}} \right|, \tag{1}$$

where x is the fraction of the snowmelt trend due to the trend in the JFM AO, r is the regression coefficient between

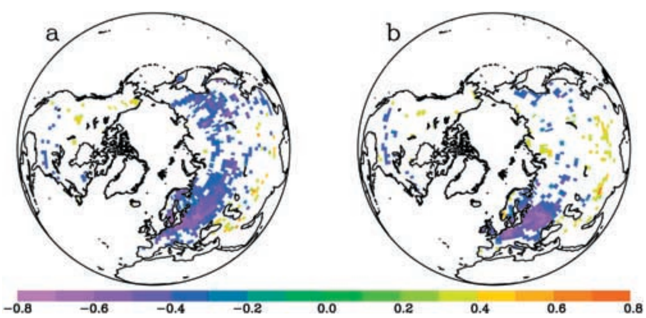

Figure 4. Correlations between the average JFM AO index and simulated snowmelt (a) and observed snowmelt (b) for 1967–2000.

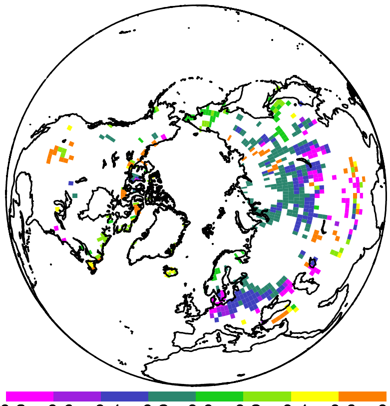

Figure 5. Simulated snowmelt trends (day year^{-1}) for 1958–2002.

the JFM AO and snowmelt, t_{AO} is the trend in the average JFM AO, and $t_{snowmelt}$ is the trend in snowmelt. When x is zero, none of the snowmelt trend results from the AO; when x is 1, the AO totally controls the snowmelt trend. The congruent trend fraction is statistically significant only where r, t_{AO}, and $t_{snowmelt}$ are statistically significant. The simulated congruent trend fraction for 1958–2002 is statistically significant in northern Europe (Figure 6), where the AO influence on snowmelt varies between 20–70%.

4. Conclusions and Discussion

[17] The winter AO exerts the strongest influence on the timing of snowmelt in northern Europe, with a weaker influence in eastern Siberia and almost no influence in North America. The trend in the winter AO towards positive polarity can statistically explain 20–70% of the simulated trends towards earlier snowmelt in northern Europe.

[18] The climate memory of snow pack allows phenomena at the synoptic time scale to influence seasonal dynamics. Climate memory occurs where a relatively slowly changing component of the land system integrates the noisy climate input into a clear, persistent response. The snow pack integrates the synoptic time scale AO signal to control the seasonal transition from winter to spring. The snow pack also responds to a trend in the synoptic scale climate:

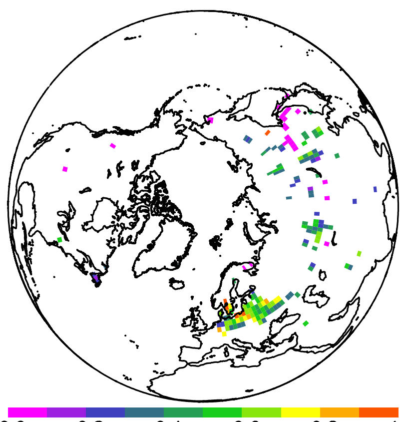

Figure 6. The fraction of simulated snowmelt trends for 1958–2002 congruent with the JFM AO trend.

a trend towards positive AO polarity can advance the date of snowmelt.

[19] **Acknowledgments.** We thank Dr. David Thompson of the Department of Atmospheric Science, Colorado State University for insight regarding the Arctic Oscillation. This research was funded by NASA Grant NCC5-621 Supplement 1, the University of California at Berkeley under NASA grant SA2805-23941, and the Colorado State University Monfort Professor Award.

References

Armstrong, R. L., and M. J. Brodzik (2002), *Northern Hemisphere EASE-Grid Weekly Snow Cover and Sea Ice Extent Version 2* [CD-ROM], Natl. Snow and Ice Data Cent., Boulder, Colo.

Bonan, G. B. (1996), A land surface model (LSM Version 1.0) for ecological, hydrological, and atmospheric studies: Technical description and users guide, *NCAR Tech. NoteNCAR/TN-417+STR*, Boulder, Colo.

Cutforth, H. W., B. G. McConkey, R. J. Woodvine, D. G. Smith, P. G. Jefferson, and O. O. Akinremi (1999), Climate change in the semiarid prairie of southwestern Saskatchewan: Late winter–early spring, *Can. J. Plant Sci.*, *79*, 343–350.

Dai, Y., et al. (2003), The common land model, *Bull. Am. Meteorol. Soc.*, *84*, 1013–1023.

Dye, D. G. (2002), Variability and trends in the annual snow-cover cycle in Northern Hemisphere land areas, *Hydrol. Proc.*, *16*, 3065–3077.

Kalnay, E., et al. (1996), The NCEP/NCAR 40-year reanalysis project, *Bull. Am. Meteorol. Soc.*, *77*, 437–471.

Schaefer, K. (2004), The influence of climate on terrestrial CO_2 fluxes, Ph.D. thesis, Colo. State Univ., Fort Collins.

Schaefer, K., A. S. Denning, N. Suits, J. Kaduk, I. Baker, S. Los, and L. Prihodko (2002), Effect of climate on interannual variability of terrestrial CO_2 fluxes, *Global Biogeochem. Cycles*, *16*(4), 1102, doi:10.1029/2002GB001928.

Sellers, P. J., D. A. Randall, G. J. Collatz, J. A. Berry, C. B. Field, D. A. Dazlich, C. Zhang, G. D. Collelo, and L. Bounoua (1996), A revised land surface parameterization of GCMs, part I: Model formulation, *J. Clim.*, *9*, 676–705.

Serreze, M. C., J. E. Walsh, F. S. Chapin, T. Osterkamp, M. Dyurgerov, V. Romanovsky, W. C. Oechel, J. Morison, T. Zhang, and R. G. Barry (2000), Observational evidence of recent change in the northern high-latitude environment, *Clim. Change*, *46*, 159–207.

Stone, R. S., E. G. Dutton, J. M. Harris, and D. Longenecker (2002), Earlier spring snowmelt in northern Alaska as an indicator of climate change, *J. Geophys. Res.*, *107*(D10), 4089, doi:10.1029/2000JD000286.

Thompson, D. W. J., and J. M. Wallace (2000), Annular Modes in the extratropical circulation. Part I: Month-to-month variability, *J. Clim.*, *13*, 1000–1016.

Thompson, D. W. J., and J. M. Wallace (2001), Regional climate impacts of the Northern Hemisphere annular mode, *Science*, *293*, 85–89.

Thompson, D. W. J., J. M. Wallace, and G. Hegerl (2000), Annular modes in the extratropical circulation. Part II: Trends, *J. Clim.*, *13*, 1018–1036.

Vaganov, E. A., M. K. Hughes, A. V. Kirdyanov, F. H. Schweingruber, and P. P. Silkin (1999), Influence of snowfall and melt timing on tree growth in subarctic Eurasia, *Nature*, *400*, 149–151.

Zhou, L. M., C. J. Tucker, R. K. Kaufmann, D. Slayback, N. V. Shabanov, and R. B. Myneni (2001), Variations in northern vegetation activity inferred from satellite data of vegetation index during 1981 to 1999, *J. Geophys. Res.*, *106*, 20,069–20,083.

A. S. Denning, O. Leonard, and K. Schaefer, Department of Atmospheric Science, Colorado State University, Fort Collins, CO 80523–1371, USA. (kevin@atmos.colostate.edu)